

# Numerical and variational solutions of the dipolar Gross-Pitaevskii equation in reduced dimensions

P. Muruganandam<sup>1,2</sup> and S. K. Adhikari<sup>1</sup>

<sup>1</sup>*Instituto de Física Teórica, UNESP - Universidade Estadual Paulista, 01.140-070 São Paulo, São Paulo, Brazil*

<sup>2</sup>*School of Physics, Bharathidasan University, Palkalaiperur Campus, Tiruchirappalli 620024, Tamilnadu, India*

We suggest a simple Gaussian Lagrangian variational scheme for the *reduced* time-dependent quasi-one- and quasi-two-dimensional Gross-Pitaevskii (GP) equations of a dipolar Bose-Einstein condensate (BEC) in cigar and disk configurations, respectively. The variational approximation for stationary states and breathing oscillation dynamics in reduced dimensions agrees well with the numerical solution of the GP equation even for moderately large short-range and dipolar nonlinearities. The Lagrangian variational scheme also provides much physical insight about soliton formation in dipolar BEC.

PACS numbers: 03.75.Hh, 03.75.Kk

## I. INTRODUCTION

The time-dependent mean-field Gross-Pitaevskii (GP) equation can accurately describe many static and dynamic properties of a harmonically trapped Bose-Einstein condensate (BEC) [1–17]. However, the numerical solution of the three-dimensional (3D) GP equation could often be a difficult task due to a large nonlinear term [18, 19]. Fortunately, in many experimental situations the 3D axially symmetric harmonic trap has extreme symmetry so that the BEC has either a cigar or a disk shape [20]. In these cases the essential statics and dynamics of a BEC take place in reduced dimensions. By integrating out the unimportant dimensional variable(s), reduced GP equations have been derived in lower dimensions [21–23], which give a faithful description of the BEC in disk and cigar shapes. For disk and cigar shapes the reduced GP equation is written in two (2D) and one dimensions (1D), respectively. The numerical solution of such 2D, or 1D equation, although simpler than that of the original 3D equation, remain complex due to the nonlinear nature of the GP equation. Hence, for small values of the nonlinearity parameter, a Gaussian variational approximation is much useful for the solution of these equations [24].

The alkali metal atoms used in early BEC experiments have negligible dipole moment. However, most bosonic atoms and molecules have large dipole moments and a <sup>52</sup>Cr [25–28], and <sup>164</sup>Dy [29, 30] BEC with a larger long-range dipolar interaction superposed on the short-range atomic interaction, has been realized. Other atoms, like <sup>166</sup>Er [31, 32], and molecules, such as <sup>7</sup>Li-<sup>133</sup>Cs [33], with much larger dipole moment are being considered for BEC experiments. A 3D GP equation for a dipolar BEC with a nonlocal nonlinear interaction has been suggested [25] and successfully used to describe many properties of these condensates [34–42].

The applicability of the nonlocal GP equation to the case of dipolar BEC has been a subject of intensive study [25]. After a detailed analysis, You and Yi [36, 37] concluded that the GP equation is valid for the dipolar BEC.

Further support on the validity of this equation came from the study of Bortolotti *et al.* [43, 44]. They compared the solution of the dipolar GP equation with the results of diffusive Monte Carlo calculations and found good agreement between the two. However, the 3D GP equation for a dipolar BEC with the nonlocal dipolar interaction has a complex structure and its numerical solution, involving the Fourier transformation of the dipolar nonlinear term to momentum space [35–37], is even more challenging than that of the GP equation of a non-dipolar BEC.

Here we reconsider the dimensional reduction [45, 46] of the GP equation to 1D form for cigar-shaped dipolar BEC and obtain the precise 1D potential with a dipolar contact-interaction term. Previous derivations [45, 46] of the 1D reduced equation for dipolar BEC did not include the proper contact-interaction term, lacking which the 1D model will not provide a correct description of the full 3D system. We also consider the reduced 2D GP equation [47, 48] for a disk-shaped dipolar BEC. Though these reduced GP equations for dipolar BEC are computationally less expensive than their 3D counterparts, the numerical solution procedure remains complicated due to repeated forward and backward Fourier transformations of the non-local dipolar term. As an alternative, here we suggest time-dependent Gaussian Lagrangian variational approximation of the 1D and 2D reduced equations. A direct attempt to derive the variational Lagrangian density of the reduced equations is not straightforward due to nonlocal integrals with error functions. We present an indirect evaluation of the Lagrangian density avoiding the above complex procedure. Thus, the present variational approximation involves algebraical quantities without requiring any Fourier transformation to momentum space.

In case of dipolar BEC of Cr and Dy atoms we consider the numerical solution of the 3D and the reduced 1D and 2D GP equations for cigar and disk shapes to demonstrate the appropriateness of the solution of the reduced equations. The variational approximation of the reduced equations provided results for density, root-mean-square (rms) size, chemical potential, and breathing oscillation

dynamics in good agreement with the numerical solution of the reduced and full 3D GP equations.

## II. ANALYTICAL FORMULATION

### A. 3D GP Equation

We study a dipolar BEC of  $N$  atoms, each of mass  $m$ , using the dimensionless GP equation [26–28]

$$i\frac{\partial\phi(\mathbf{r},t)}{\partial t} = \left[ -\frac{1}{2}\nabla^2 + V(\mathbf{r}) + 4\pi aN|\phi(\mathbf{r},t)|^2 + N \int U_{dd}(\mathbf{r}-\mathbf{r}')|\phi(\mathbf{r}',t)|^2 d^3r' \right] \phi(\mathbf{r},t), \quad (1)$$

with dipolar interaction  $U_{dd}(\mathbf{R}) = 3a_{dd}(1-3\cos^2\theta)/R^3$ ,  $\mathbf{R} = \mathbf{r} - \mathbf{r}'$ . Here  $V(\mathbf{r})$  is the confining axially symmetric harmonic potential,  $\phi(\mathbf{r},t)$  the wave function at time  $t$  with normalization  $\int |\phi(\mathbf{r},t)|^2 d\mathbf{r} = 1$ ,  $a$  the atomic scattering length,  $\theta$  the angle between  $\mathbf{R}$  and the polarization direction  $z$ . The constant  $a_{dd} = \mu_0\bar{\mu}^2m/(12\pi\hbar^2)$  is a length characterizing the strength of dipolar interaction and its experimental value for  $^{52}\text{Cr}$  is  $15a_0$  [26–28], with  $a_0$  the Bohr radius,  $\bar{\mu}$  the (magnetic) dipole moment of a single atom, and  $\mu_0$  the permeability of free space. In equation (1) length is measured in units of characteristic harmonic oscillator length  $l \equiv \sqrt{\hbar/m\omega}$ , angular frequency of trap in units of  $\omega$ , time  $t$  in units of  $\omega^{-1}$ , and energy in units of  $\hbar\omega$ . The axial and radial angular frequencies of the trap are  $\Omega_z\omega$  and  $\Omega_\rho\omega$ , respectively. The dimensionless 3D harmonic trap is

$$V(\mathbf{r}) = \frac{1}{2}\Omega_\rho^2\rho^2 + \frac{1}{2}\Omega_z^2z^2, \quad (2)$$

where  $\mathbf{r} \equiv (\bar{\rho}, z)$ , with  $\bar{\rho}$  the radial coordinate and  $z$  the axial coordinate.

The Lagrangian density of equation (1) is given by

$$\mathcal{L} = \frac{i}{2}(\phi\phi_t^* - \phi_t^*\phi) + \frac{|\nabla\phi|^2}{2} + V(\mathbf{r})|\phi|^2 + 2\pi aN|\phi|^4 + \frac{N}{2}|\phi|^2 \int U_{dd}(\mathbf{r}-\mathbf{r}')|\phi(\mathbf{r}')|^2 d^3r'. \quad (3)$$

We use the Gaussian ansatz [24, 35–37]

$$\phi(\mathbf{r},t) = \frac{\pi^{-3/4}}{w_\rho\sqrt{w_z}} \exp\left(-\frac{\rho^2}{2w_\rho^2} - \frac{z^2}{2w_z^2} + i\alpha\rho^2 + i\beta z^2\right) \quad (4)$$

for a variational calculation, where  $w_\rho$  and  $w_z$  are time-dependent radial and axial widths, and  $\alpha$  and  $\beta$  time-dependent phases. The effective Lagrangian  $L \equiv \int \mathcal{L} d^3r$  (per particle) becomes

$$L = \left( w_\rho^2\dot{\alpha} + \frac{w_z^2\dot{\beta}}{2} \right) + \frac{\Omega_\rho^2 w_\rho^2}{2} + \frac{\Omega_z^2 w_z^2}{4} + \frac{1}{2w_\rho^2} + \frac{1}{4w_z^2} + 2w_\rho^2\alpha^2 + w_z^2\beta^2 + \frac{N}{(\sqrt{2\pi}w_\rho^2w_z)} [a - a_{dd}f(\kappa)], \quad (5)$$

with

$$f(\kappa) = \frac{1 + 2\kappa^2 - 3\kappa^2 d(\kappa)}{(1 - \kappa^2)}, \quad (6)$$

$$d(\kappa) = \frac{\text{atanh}\sqrt{1 - \kappa^2}}{\sqrt{1 - \kappa^2}}, \quad \kappa = \frac{w_\rho}{w_z}. \quad (7)$$

The Euler-Lagrange equations for variational parameters  $w_\rho, w_z, \alpha$  and  $\beta$  yield the following equations for widths  $w_\rho$  and  $w_z$

$$\ddot{w}_\rho + \Omega_\rho^2 w_\rho = \frac{1}{w_\rho^3} + \frac{N}{\sqrt{2\pi}} \frac{[2a - a_{dd}g(\kappa)]}{w_\rho^3 w_z}, \quad (8)$$

$$\ddot{w}_z + \Omega_z^2 w_z = \frac{1}{w_z^3} + \frac{2N}{\sqrt{2\pi}} \frac{[a - a_{dd}c(\kappa)]}{w_\rho^2 w_z^2}, \quad (9)$$

with

$$g(\kappa) = \frac{2 - 7\kappa^2 - 4\kappa^4 + 9\kappa^4 d(\kappa)}{(1 - \kappa^2)^2}, \quad (10)$$

$$c(\kappa) = \frac{1 + 10\kappa^2 - 2\kappa^4 - 9\kappa^2 d(\kappa)}{(1 - \kappa^2)^2}. \quad (11)$$

The chemical potential  $\mu$  for a stationary state is

$$\mu = \frac{1}{2w_\rho^2} + \frac{1}{4w_z^2} + \frac{2N[a - a_{dd}f(\kappa)]}{\sqrt{2\pi}w_z w_\rho^2} + \frac{\Omega_\rho^2 w_\rho^2}{2} + \frac{\Omega_z^2 w_z^2}{4}. \quad (12)$$

### B. 1D reduction

For a cigar-shaped dipolar BEC with a strong radial trap ( $\Omega_\rho > \Omega_z$ ) one can write the following effective 1D equation (details given in Appendix)

$$i\frac{\partial\phi_{1D}(z,t)}{\partial t} = \left[ -\frac{\partial_z^2}{2} + \frac{\Omega_z^2 z^2}{2} + \frac{2aN}{d_\rho^2} |\phi_{1D}|^2 + \frac{2a_{dd}N}{d_\rho^2} \times \int_{-\infty}^{\infty} \frac{dk_z}{2\pi} e^{ik_z z} \tilde{n}(k_z) s_{1D} \left( \frac{k_z d_\rho}{\sqrt{2}} \right) \right] \phi_{1D}(z,t), \quad (13)$$

where  $s_{1D}$  is defined by equation (A9) and  $d_\rho \equiv 1/\sqrt{\Omega_\rho}$  is the radial harmonic oscillator length.

To solve equation (13), we use the Gaussian variational ansatz

$$\phi_{1D}(z) = \frac{\pi^{-1/4}}{\sqrt{w_z}} \exp\left[-\frac{z^2}{2w_z^2} + i\beta z^2\right]. \quad (14)$$

From equation (A2) we see that the variational 1D ansatz (14) corresponds to the following 3D wave function

$$\phi(\mathbf{r},t) = \frac{\pi^{-3/4}}{d_\rho\sqrt{w_z}} \exp\left(-\frac{\rho^2}{2d_\rho^2} - \frac{z^2}{2w_z^2} + i\beta z^2\right). \quad (15)$$

The present variational wave function (15) is a special case of the 3D variational wave function (4) with  $w_\rho = d_\rho$  and  $\alpha = 0$ . Hence, the 1D variational Lagrangian can be

written from the 3D Lagrangian (5), (using  $w_\rho = d_\rho$  and  $\alpha = 0$ ), as

$$L_{1D} = \frac{w_z^2 \dot{\beta}}{2} + \frac{1}{4w_z^2} + w_z^2 \beta^2 + \frac{\Omega_z^2 w_z^2}{4} + \frac{N}{\sqrt{2\pi d_\rho^2 w_z}} [a - a_{dd} f(\kappa_0)]; \quad \kappa_0 = \frac{d_\rho}{w_z}, \quad (16)$$

where we have removed the constant terms. This inductive derivation of the 1D Lagrangian (16) avoids the construction of Lagrangian density involving error functions in the 1D potential (A10) and subsequent integration to obtain the Lagrangian. The Euler-Lagrange equation for the variational parameter  $w_z$  of Lagrangian (16) is

$$\ddot{w}_z + \Omega_z^2 w_z = \frac{1}{w_z^3} + \frac{2N[a - a_{dd} c(\kappa_0)]}{\sqrt{2\pi w_z^2 d_\rho^2}}. \quad (17)$$

The variational chemical potential is given by

$$\mu = \frac{1}{4w_z^2} + \frac{2N[a - a_{dd} f(\kappa_0)]}{\sqrt{2\pi w_z d_\rho^2}} + \frac{\Omega_z^2 w_z^2}{4}. \quad (18)$$

Not only are the above variational results simple and yield a good approximation to the 1D GP equation, much physical insight about the system can be obtained from the variational Lagrangian (16). In a quasi-1D system, the axial width is much larger than the transverse oscillator length:  $w_z \gg d_\rho$ . Consequently,  $\kappa_0 \rightarrow 0$  and  $f(\kappa_0) \rightarrow 1$ . From equation (16), we see that the interaction term becomes in this limit  $N(a - a_{dd})/(\sqrt{2\pi} d_\rho^2 w_z)$ . In equation (13), the dipolar term involves a nonlocal integral. However, the variational approximation suggests that the effect of the dipolar interaction integral is to reduce the contact interaction term in equation (13) replacing the scattering length  $a$  by  $(a - a_{dd})$ . Immediately, one can conclude that the system effectively becomes attractive for  $a_{dd} > a$ . So one can have the formation of bright soliton even for positive (repulsive) scattering length  $a$ , provided that  $a_{dd} > a$ .

### C. 2D reduction

In the disk-shape, with a strong axial trap ( $\Omega_z > \Omega_\rho$ ), the dipolar BEC is assumed to be in the ground state  $\phi(z) = \exp(-z^2/2d_z^2)/(\pi d_z^2)^{1/4}$  of the axial trap and the wave function  $\phi(\mathbf{r})$  can be written as [47, 48]

$$\phi(\mathbf{r}) = \frac{1}{(\pi d_z^2)^{1/4}} \exp\left(-\frac{z^2}{2d_z^2}\right) \phi_{2D}(x, y), \quad (19)$$

where  $\phi_{2D}(x, y)$  is the 2D wave function and  $d_z = \sqrt{1/\Omega_z}$ . Using ansatz (19) in equation (1), the  $z$  dependence can be integrated out to obtain the following

effective 2D equation [47, 48]

$$i \frac{\partial \phi_{2D}(\vec{\rho}, t)}{\partial t} = \left[ -\frac{\nabla_\rho^2}{2} + \frac{\Omega_\rho^2 \rho^2}{2} + \frac{4\pi a N}{\sqrt{2\pi} d_z} |\phi_{2D}|^2 + \frac{4\pi a_{dd} N}{\sqrt{2\pi} d_z} \times \int \frac{d^2 k_\rho}{(2\pi)^2} \exp(i\mathbf{k}_\rho \cdot \vec{\rho}) \tilde{n}(\mathbf{k}_\rho) h_{2D}\left(\frac{k_\rho d_z}{\sqrt{2}}\right) \right] \phi_{2D}(\vec{\rho}, t), \quad (20)$$

$$\tilde{n}(\mathbf{k}_\rho) = \int \exp(i\mathbf{k}_\rho \cdot \vec{\rho}) |\phi_{2D}(\vec{\rho})|^2 d\vec{\rho}, \quad (21)$$

where  $h_{2D}(\xi) = 2 - 3\sqrt{\pi}\xi e^{\xi^2} \text{erfc}(\xi)$  [48],  $\mathbf{k}_\rho \equiv (k_x, k_y)$ , and the dipolar term is written in Fourier space.

To solve equation (20), we use the Gaussian ansatz

$$\phi_{2D}(\rho) = \frac{1}{w_\rho \sqrt{\pi}} \exp\left(-\frac{\rho^2}{2w_\rho^2} + i\alpha \rho^2\right). \quad (22)$$

From equation (19) we see that the 2D wave function (22) corresponds to the following 3D wave function

$$\phi(\mathbf{r}, t) = \frac{\pi^{-3/4}}{w_\rho \sqrt{d_z}} \exp\left(-\frac{\rho^2}{2w_\rho^2} - \frac{z^2}{2d_z^2} + i\alpha \rho^2\right). \quad (23)$$

The present variational wave function (23) is a special case of the 3D variational wave function (4) with  $w_z = d_z$  and  $\beta = 0$ . Hence, the 2D variational Lagrangian can be written from the 3D Lagrangian (5) as

$$L_{2D} = w_\rho^2 \dot{\alpha} + \frac{w_\rho^2 \Omega_\rho^2}{2} + \frac{1}{2w_\rho^2} + 2w_\rho^2 \alpha^2 + \frac{N}{\sqrt{2\pi} w_\rho^2 d_z} [a - a_{dd} f(\bar{\kappa})]; \quad \bar{\kappa} = \frac{w_\rho}{d_z}, \quad (24)$$

where we have removed the constant terms. The Euler-Lagrange variational equation for width  $w_\rho$  becomes

$$\ddot{w}_\rho + w_\rho \Omega_\rho^2 = \frac{1}{w_\rho^3} + \frac{N}{\sqrt{2\pi}} \frac{[2a - a_{dd} g(\bar{\kappa})]}{w_\rho^3 d_z}. \quad (25)$$

The chemical potential  $\mu$  for a stationary state is

$$\mu = \frac{1}{2w_\rho^2} + \frac{2N[a - a_{dd} f(\bar{\kappa})]}{\sqrt{2\pi} d_z w_\rho^2} + \frac{w_\rho^2 \Omega_\rho^2}{2}. \quad (26)$$

In a quasi-2D system, the radial width is much larger than the axial oscillator length:  $w_\rho \gg d_z$ . Consequently,  $\bar{\kappa} \rightarrow \infty$  and  $f(\bar{\kappa}) \rightarrow -2$ . From equation (24), we see that the interaction term becomes in this limit  $N(a + 2a_{dd})/(\sqrt{2\pi} w_\rho^2 d_z)$ . The variational approximation suggests that the effect of the dipolar interaction in equation (20) is to increase the contact interaction term replacing  $a$  by  $(a + 2a_{dd})$ . Hence, for positive  $a$ , there cannot be any bright soliton in 2D, which was found from a solution of the 2D GP equation (20) and Bogoliubov theory [49]. However, effectively the sign of the dipolar term in the GP equation can be changed by rotating the external field that orients the dipoles much faster than any other relevant time scale in the system [50]. In

this fashion Nath *et al.* [50] suggest changing the dipole interaction term by a factor of  $-1/2$ , which changes the effective scattering length in the Lagrange variational approximation to  $(a - a_{dd})$ , (as discussed in the 1D case above,) leading to the formation of bright 2D solitons for  $a_{dd} > a$ . These solitons were obtained by Nath *et al.* from a solution of the 2D GP equation (20).

### III. NUMERICAL RESULTS

We solve the 1D, 2D, and 3D GP equations employing imaginary- and real-time propagation with Crank-Nicolson method [18, 19]. The dipolar interaction is evaluated by fast Fourier transform [35, 36].

We present results for  $^{52}\text{Cr}$  and  $^{164}\text{Dy}$  atoms. The  $^{52}\text{Cr}$  has a moderate dipole moment with  $a_{dd} = 15a_0$  [26–28], while the  $^{164}\text{Dy}$  atom has a large dipole moment with  $a_{dd} = 130a_0$  [29, 30]. In both cases we present results for dipolar BEC of up to 10,000 atoms for  $0 < a < 10$  nm and choose the frequency  $\omega$  such that the oscillator length  $l = 1\mu\text{m}$ .

First, we present the results for density profiles obtained from a solution of the reduced 1D and 2D equation and compare with the full 3D results. It is known that the densities obtained from the reduced equations agree well with the full 3D density, as the nonlinearity tends to zero and/or the trap asymmetry is extreme [21]. Hence in this study we consider a moderately small trap asymmetry and a relatively large nonlinearity of experimental interest. In the cigar (1D) case we consider  $^{52}\text{Cr}$  atoms with  $a = 6$  nm, and in the disk (2D) case we consider  $^{164}\text{Dy}$  atoms with  $a = 6$  nm.

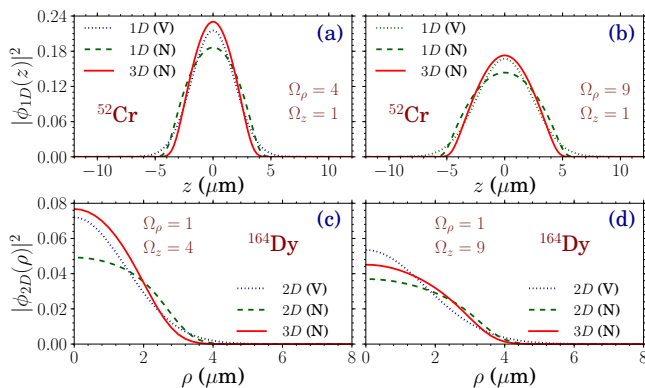


FIG. 1. Linear density of a cigar-shaped  $^{52}\text{Cr}$  dipolar BEC of 1,000 atoms of  $a = 6$  nm, with trap parameters  $\Omega_z = 1$  and (a)  $\Omega_\rho = 4$ , and (b)  $\Omega_\rho = 9$  from a numerical (N) solution of the 3D equation (1) and 1D equation (13), and its variational (V) result. Radial density of a disk-shaped  $^{164}\text{Dy}$  dipolar BEC of 1,000 atoms of  $a = 6$  nm, with trap parameters  $\Omega_\rho = 1$  and (c)  $\Omega_z = 4$ , and (d)  $\Omega_z = 9$  from a numerical solution of the 3D equation (1) and 2D equation (20), and its variational result.

In Figs. 1 (a) and (b), we plot results for linear density of a cigar-shaped  $^{52}\text{Cr}$  dipolar BEC of 1,000 atoms as calculated from the numerical solution of the 3D equation (1) and the 1D equation (13) and its variational result (17) for  $\Omega_z = 1$  and  $\Omega_\rho = 4$  and 9. We find, as the trap asymmetry increases by changing  $\Omega_\rho$  from 4 to 9, the agreement between 3D and 1D models improves. In Figs. 1 (c) and (d), we plot results for radial density of a disk-shaped  $^{164}\text{Dy}$  dipolar BEC of 1,000 atoms as calculated from the numerical solution of the 3D equation (1) and the 2D equation (20) and its variational approximation (25) for  $\Omega_\rho = 1$  and  $\Omega_z = 4$  and 9. We find that, with the increase of the trap asymmetry from  $\Omega_z = 4$  to 9, the agreement between the 3D and 2D models enhances. In all cases the variational results of the reduced 1D and 2D equations are in good agreement with those of the full 3D model.

After having established the appropriateness of the reduced 1D and 2D equations in the cigar and disk shapes, it is realized that although the numerical solution of these reduced GP equations are simpler than that of the full 3D GP equation, they are still complicated due to the presence of the nonlocal dipolar interaction. The variational approximation of these equations presented here is relatively simple and could be used for approximate solution of these equations. Now we test the variational results of the reduced 1D and 2D equations by comparing with the numerical solution of these equations.

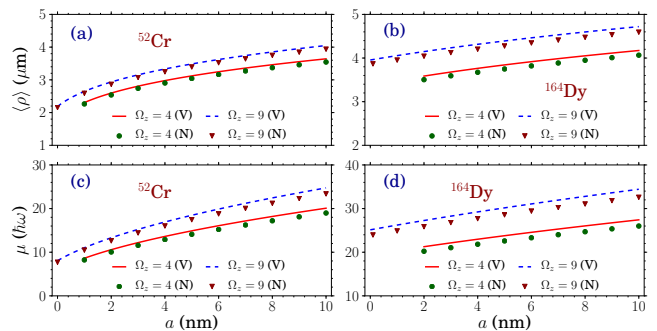


FIG. 2. The numerical (N) and variational (V) rms size  $\langle \rho \rangle$  versus scattering length  $a$  of a disk-shaped dipolar BEC of 10,000 (a)  $^{52}\text{Cr}$  and (b)  $^{164}\text{Dy}$  atoms for trap parameters  $\Omega_\rho = 1$  and  $\Omega_z = 4$  and 9 from a solution of the reduced 2D GP equation (20). The corresponding chemical potential  $\mu$  in these cases for (c)  $^{52}\text{Cr}$  and (d)  $^{164}\text{Dy}$  atoms.

In Figs. 2 we present the results for rms size  $\langle \rho \rangle$  and chemical potential  $\mu$  of a disk-shaped  $^{52}\text{Cr}$  and  $^{164}\text{Dy}$  dipolar BEC of 10,000 atoms with the trap parameters  $\Omega_\rho = 1$  and  $\Omega_z = 4$  and 9 for  $0 < a < 10$  nm as calculated from numerical and variational approaches of the reduced 2D equation (20). In Figs. 3 we exhibit the results for rms size  $\langle z \rangle$  and chemical potential  $\mu$  of a cigar-shaped  $^{52}\text{Cr}$  and  $^{164}\text{Dy}$  dipolar BEC of 10,000 atoms with the trap parameters  $\Omega_z = 1$  and  $\Omega_\rho = 4$  and 9 for  $0 < a < 20$  nm as calculated from numerical and

variational approaches of the reduced 1D equation (13).

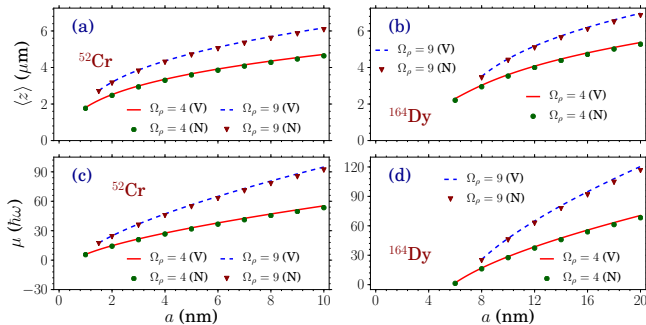


FIG. 3. The numerical (N) and variational (V) rms length  $\langle z \rangle$  versus scattering length  $a$  of a cigar-shaped dipolar BEC of 10,000 (a)  $^{52}\text{Cr}$  and (b)  $^{164}\text{Dy}$  atoms for trap parameters  $\Omega_z = 1$  and  $\Omega_\rho = 4$  and 9 from a solution of the reduced 1D GP equation (13). The corresponding chemical potential  $\mu$  in these cases for (c)  $^{52}\text{Cr}$  and (d)  $^{164}\text{Dy}$  atoms.

The dipolar interaction changes from strongly attractive in the extreme cigar shape ( $\Omega_\rho \gg \Omega_z$ ) to strongly repulsive in the extreme disk shape ( $\Omega_\rho \ll \Omega_z$ ) and its effect is minimum (nearly zero) for  $\Omega_\rho$  slightly less than  $\Omega_z$ . In Fig. 2 the dipolar interaction is slightly attractive for  $\Omega_z = 4$  and  $\Omega_\rho = 1$ . Hence in the absence of any short-range interaction ( $a = 0$ ), the system will collapse and no stable solution of the GP equation can be obtained. For Cr atoms the dipolar interaction is weak, and for  $a \geq 1$  nm, the short-range repulsion for 10,000 atoms surpluses the dipolar attraction and a stable state can be obtained for  $\Omega_z = 4$ . For Dy atoms the dipolar interaction is stronger, and a stable state can be obtained only for  $a \geq 2$  nm for  $\Omega_z = 4$ . For  $\Omega_z = 9$ , the dipolar interaction for both Cr and Dy atoms are repulsive and a stable state is obtained in this case for  $a > 0$ . In Fig. 3 the dipolar interaction is attractive for both  $\Omega_\rho = 4$  and 9. Hence the dipolar BEC can be stable only for scattering length  $a$  greater than a critical value. This is why the curves in this figure start above this critical value. This critical value is larger for Dy atoms and  $\Omega_\rho = 9$  compared to that of Cr atoms and  $\Omega_\rho = 4$  as can be found in Fig. 3. As there is no real collapse in 1D models with cubic nonlinearity; for confirming the collapse correctly one must solve the full 3D GP equation.

Next we study, by numerical and variational solutions of the reduced 1D and 2D equations, the dynamics of breathing oscillation of the four dipolar BEC of cigar- and disk-shaped Cr and Dy atoms shown in Figs. 1 started by a small change of the scattering length. This can be implemented experimentally by a Feshbach resonance [51]. In Fig. 4 this dynamics is shown for a cigar-shaped Cr dipolar BEC of 1,000 atoms for (a)  $\Omega_\rho = 4$  and (b)  $\Omega_\rho = 9$  from a solution of the reduced 1D equation, and for a disk-shaped Dy dipolar BEC of 1,000 atoms for (c)  $\Omega_z = 4$  and (d)  $\Omega_z = 9$  from a solution of the reduced 2D equation. In these figures we also show the results from

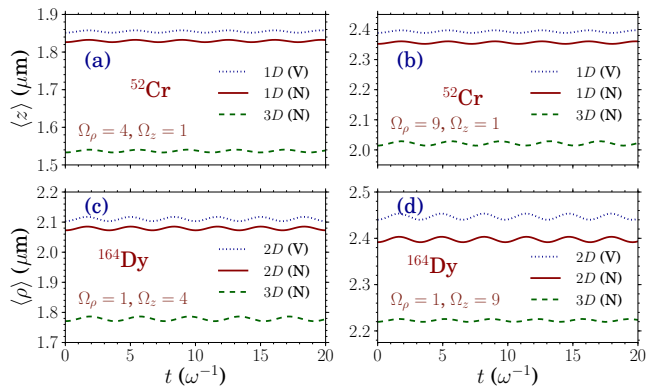


FIG. 4. The rms sizes  $\langle z \rangle$  of a cigar-shaped Cr dipolar BEC of 1,000 atoms versus time  $t$  for (a)  $\Omega_\rho = 4$  and (b) 9 from a numerical (N) and variational (V) results of the reduced 1D equation. The rms sizes  $\langle \rho \rangle$  of a disk-shaped Dy dipolar BEC of 1,000 atoms versus time  $t$  for (c)  $\Omega_z = 4$  and (d) 9. The oscillation was initiated by jumping the scattering length  $a$  from 6 nm to 6.15 nm for Cr (6.3 nm for Dy) at  $t = 0$  from a solution of the reduced 2D equation.

a numerical solution of the 3D Eq. (1). The agreement between the numerical and variational results is good in all cases. We also calculated the angular frequencies of these oscillations. In case of Cr in Figs. 4 (a) and (b), the axial frequencies are 1.75 (variational, 1D), 1.76 (numerical, 1D) and 1.63 (numerical, 3D), and in case of Dy in Figs. 4 (c) and (d), the radial frequencies are 1.93 (variational, 2D), 1.89 (numerical, 2D) and 1.76 (numerical, 3D). For quasi-linear systems, these angular frequencies are expected to be 2 [52]. The deviation from this value is due to the large nonlinearity of the dipolar BECs considered here.

#### IV. CONCLUSION

The usual GP equation provides a good description of statics and dynamics of a normal nondipolar BEC. For a dipolar BEC the numerical solution of the GP equation is a difficult task due to the nonlocal dipolar interaction. For a cigar- and disk-shaped dipolar BEC, the reduced 1D and 2D equations provide an alternative to the full 3D equation. Nevertheless, the solution of these reduced equations is also challenging involving Fourier and inverse Fourier transformations. As an alternative, we suggest a time-dependent variational scheme for these reduced equations, not requiring any Fourier transformation. The variational approximation of these reduced equations provides results for stationary cigar- and disk-shaped dipolar BEC as well as for breathing oscillation of the same in good agreement with the numerical solution of the respective GP equations. This is illustrated for large Cr and Dy dipolar BECs of 10,000 atoms and large atomic scattering lengths  $a$  up to 20 nm. We also study

the breathing oscillation of a bright soliton of 1,000 Cr atoms using the numerical solution of the 3D equation as well as the numerical and variational approaches to the 1D equation. A typical dipolar BEC considered here corresponds to a large short-range cubic nonlinearity of about  $4\pi aN \approx 1250$  for  $a = 10$  nm and  $N = 10,000$  and a large dipolar nonlinearity of  $4\pi a_{dd} \approx 865$  for Dy atoms for  $a_{dd} = 130a_0$  and  $N = 10,000$ . The variational approximations considered here provided good results for such large nonlinearities and should be useful for analyzing the statics and dynamics of realistic dipolar BECs under appropriate experimental conditions.

### ACKNOWLEDGMENTS

We thank FAPESP (Brazil), CNPq (Brazil), DST (India), and CSIR (India) for partial support.

### Appendix A: 1D reduction

For a cigar-shaped dipolar BEC with a strong radial trap ( $\Omega_\rho > \Omega_z$ ), we assume that in the radial direction the dipolar BEC is confined in the ground state

$$\phi(\rho) = \exp(-(\rho^2/2d_\rho^2)/(d_\rho\sqrt{\pi})) \quad (\text{A1})$$

of the transverse trap and the wave function  $\phi(\mathbf{r}) = \phi_{1D}(z) \times \phi(\rho)$  can be written as [45, 46]

$$\phi(\mathbf{r}) = \frac{1}{\sqrt{\pi d_\rho^2}} \exp\left[-\frac{\rho^2}{2d_\rho^2}\right] \phi_{1D}(z); \quad \Omega_\rho d_\rho^2 = 1, \quad (\text{A2})$$

where  $d_\rho$  is the radial harmonic oscillator length.

The contribution of the dipole potential to energy is

$$H_{dd} = \frac{N}{2} \int d^3r \int d^3r' n(\mathbf{r}) U_{dd}(\mathbf{r} - \mathbf{r}') n(\mathbf{r}'), \quad (\text{A3})$$

$$= \frac{1}{2} \frac{N}{(2\pi)^3} \int d^3k \tilde{n}(\mathbf{k}) \tilde{U}_{dd}(\mathbf{k}) \tilde{n}(-\mathbf{k}), \quad (\text{A4})$$

where  $n(\mathbf{r}) \equiv |\phi(\mathbf{r})|^2$  is the density and in Eq. (A4) we used a convolution of the respective variables to Fourier space and where tilde denotes Fourier transformations:

[35, 36, 47, 48]

$$\tilde{U}_{dd}(\mathbf{k}) = \frac{4\pi}{3} 3a_{dd} \left[ \frac{3k_z^2}{k^2} - 1 \right], \quad (\text{A5})$$

$$\tilde{n}(\mathbf{k}) = \exp\left[-\frac{k_\rho^2 d_\rho^2}{4}\right] \tilde{n}_{1D}(k_z). \quad (\text{A6})$$

The  $k_x, k_y$  integrals in (A4) can now be done and

$$\begin{aligned} H_{dd} &= \frac{4\pi N}{3} \frac{3a_{dd}}{2} \frac{1}{2\pi} \int_{-\infty}^{\infty} dk_z \tilde{n}_{1D}(k_z) \tilde{n}_{1D}(-k_z) \frac{1}{(2\pi)^2} \\ &\times \int_{-\infty}^{\infty} \int_{-\infty}^{\infty} dk_x dk_y \left[ \frac{3k_z^2}{k_\rho^2 + k_z^2} - 1 \right] \exp\left[-\frac{k_\rho^2 d_\rho^2}{2}\right], \\ &\equiv \frac{N}{2} \frac{1}{2\pi} \int_{-\infty}^{\infty} dk_z \tilde{n}_{1D}(k_z) \tilde{n}_{1D}(-k_z) V_{1D}(k_z), \end{aligned} \quad (\text{A7})$$

where the 1D potential in Fourier space is

$$\begin{aligned} V_{1D}(k_z) &= 2a_{dd} \int_0^\infty dk_\rho k_\rho \left[ \frac{3k_z^2}{k_\rho^2 + k_z^2} - 1 \right] \exp\left[-\frac{k_\rho^2 d_\rho^2}{2}\right], \\ &\equiv \frac{2a_{dd}}{d_\rho^2} s_{1D}\left(\frac{k_z d_\rho}{\sqrt{2}}\right), \end{aligned} \quad (\text{A8})$$

$$s_{1D}(\zeta) = \int_0^\infty du \left[ \frac{3\zeta^2}{u + \zeta^2} - 1 \right] e^{-u}. \quad (\text{A9})$$

The 1D potential in configuration space is

$$\begin{aligned} U_{dd}^{1D}(Z) &= \frac{1}{2\pi} \int_{-\infty}^{\infty} dk_z e^{ik_z z} V_{1D}(k_z) \\ &= \frac{6a_{dd}}{(\sqrt{2}d_\rho)^3} \left[ \frac{4}{3} \delta(\sqrt{t}) + 2\sqrt{t} - \sqrt{\pi}(1+2t)e^t \operatorname{erfc}(\sqrt{t}) \right], \end{aligned} \quad (\text{A10})$$

where  $t = [Z/(\sqrt{2}d_\rho)]^2$ ,  $Z = |z - z'|$ . Similar, but not identical, 1D reduced potential was derived in [45, 46], where the  $\delta$ -function term was absent. To derive the effective 1D equation for the cigar-shaped dipolar BEC, we substitute the ansatz (A2) in Eq. (1), multiply by the ground-state wave function  $\phi(\rho)$  and integrate in  $\rho$  to get the 1D equation

$$\begin{aligned} i \frac{\partial \phi_{1D}(z, t)}{\partial t} &= \left[ -\frac{\partial_z^2}{2} + \frac{\Omega_z^2 z^2}{2} + \frac{2aN}{d_\rho^2} |\phi_{1D}|^2 \right. \\ &\left. + \frac{2a_{dd}N}{d_\rho^2} \int_{-\infty}^{\infty} \frac{dk_z}{2\pi} e^{ik_z z} \tilde{n}(k_z) s_{1D}\left(\frac{k_z d_\rho}{\sqrt{2}}\right) \right] \phi_{1D}(z, t), \end{aligned} \quad (\text{A11})$$

$$\begin{aligned} &\equiv \left[ -\frac{\partial_z^2}{2} + \frac{\Omega_z^2 z^2}{2} + \frac{2aN|\phi_{1D}|^2}{d_\rho^2} \right. \\ &\left. + N \int_{-\infty}^{\infty} U_{dd}^{1D}(Z) |\phi_{1D}(z', t)|^2 dz' \right] \phi_{1D}(z, t). \end{aligned} \quad (\text{A12})$$

- 
- [1] F. Dalfovo, S. Giorgini, L. P. Pitaevskii, and S. Stringari, *Rev. Mod. Phys.* **71**, 463 (1999).
- [2] P. W. Courteille, V. S. Bagnato, and V. I. Yukalov, *Laser Phys.* **11**, 659 (2001).
- [3] Y. Cheng and S. K. Adhikari, *Laser Phys. Lett.* **7**, 824 (2010).
- [4] V. I. Yukalov, *Laser Phys. Lett.* **8**, 485 (2011).
- [5] V. I. Yukalov and V. S. Bagnato, *Laser Phys. Lett.* **6**, 399 (2009).
- [6] V. I. Yukalov and E. P. Yukalova, *Laser Phys. Lett.* **6**, 235 (2009).
- [7] J. A. Seman, E.A.L. Henn, R. F. Shiozaki, G. Roati, F. J. Poveda-Cuevas, K. M. F. Magalhães, V.I. Yukalov, M. Tsubota, M. Kobayashi, K. Kasamatsu, and V. S. Bagnato, *Laser Phys. Lett.* **8**, 691 (2011).
- [8] H. W. Xiong and B. Wu, *Laser Phys. Lett.* **8**, 398 (2011).
- [9] V. I. Yukalov, *Laser Phys. Lett.* **7**, 467 (2010).
- [10] L. Salasnich, F. Ancilotto, and F. Toigo, *Laser Phys. Lett.* **7**, 78 (2010).
- [11] V. I. Yukalov and E. P. Yukalova, *Laser Phys.* **21**, 1448 (2011).
- [12] L. Tomio, M. T. Yamashita, T. Frederico, and F. Bringas, *Laser Phys.* **21**, 1464 (2011).
- [13] T. D. Graß, F. E. A. dos Santos, and A. Pelster, *Laser Phys.* **21**, 1459 (2011).
- [14] L. Chen, S. W. Bi, and B. Z. Lu, *Laser Phys.* **21**, 1202 (2011).
- [15] Z. -B. Lu, J. -S. Chen, and J. -R. Li, *Laser Phys.* **20**, 910 (2010).
- [16] B. S. Marangoni, C. R. Menegatti, and L. G. Marcassa, *Laser Phys.* **20**, 557 (2010).
- [17] I. Vidanović, A. Balaž, H. Al-Jibbouri, and A. Pelster, *Phys. Rev. A* **84**, 013618 (2011).
- [18] P. Muruganandam and S. K. Adhikari, *Comput. Phys. Commun.* **180**, 1888 (2009).
- [19] S. K. Adhikari and P. Muruganandam, *J. Phys. B* **35**, 2831 (2002).
- [20] A. Görlitz, J. M. Vogels, A. E. Leanhardt, C. Raman, T. L. Gustavson, J. R. Abo-Shaer, A. P. Chikkatur, S. Gupta, S. Inouye, T. Rosenband, and W. Ketterle, *Phys. Rev. Lett.* **87**, 130402 (2001).
- [21] L. Salasnich, A. Parola, and L. Reatto, *Phys. Rev. A* **65**, 043614 (2002).
- [22] C. A. G. Buitrago and S. K. Adhikari, *J. Phys. B* **42**, 215306 (2009).
- [23] A. Muñoz Mateo and V. Delgado, *Phys. Rev. A* **77**, 013617 (2008).
- [24] V. M. Pérez-García, H. Michinel, J. I. Cirac, M. Lewenstein, and P. Zoller, *Phys. Rev. A* **56**, 1424 (1997).
- [25] T. Lahaye, C. Menotti, L. Santos, M. Lewenstein and T. Pfau, *Rep. Prog. Phys.* **72**, 126401 (2009).
- [26] T. Koch, T. Lahaye, J. Metz, B. Fröhlich, A. Griesmaier and T. Pfau *Nature Phys.* **4**, 218 (2008).
- [27] T. Lahaye, T. Koch, B. Fröhlich, M. Fattori, J. Metz, A. Griesmaier, S. Giovanazzi and T. Pfau, *Nature* **448**, 672 (2007).
- [28] A. Griesmaier, J. Stuhler, T. Koch, M. Fattori, T. Pfau, and S. Giovanazzi, *Phys. Rev. Lett.* **97**, 250402 (2006).
- [29] S. H. Youn, M. W. Lu, U. Ray, and B. L. Lev, *Phys. Rev. A* **82**, 043425 (2010).
- [30] M. Lu, N. Q. Burdick, Seo Ho Youn, and B. L. Lev, *Phys. Rev. Lett.* **107**, 190401 (2011).
- [31] C. I. Hancox, S. C. Doret, M. T. Hummon, L. J. Luo, and J. M. Doyle, *Nature* **431**, 281 (2004).
- [32] J. J. McClelland and J. L. Hanssen, *Phys. Rev. Lett.* **96**, 143005 (2006).
- [33] J. Deiglmayr, A. Grochola, M. Repp, K. Mörtlbauer, C. Glück, J. Lange, O. Dulieu, R. Wester, and M. Weidemüller, *Phys. Rev. Lett.* **101**, 133004 (2008).
- [34] I. Tikhonenkov, B. A. Malomed, and A. Vardi, *Phys. Rev. Lett.* **100**, 090406 (2008).
- [35] K. Góral and L. Santos, *Phys. Rev. A* **66**, 023613 (2002).
- [36] S. Yi and L. You, *Phys. Rev. A* **63**, 053607 (2001).
- [37] S. Yi and L. You, *Phys. Rev. A* **61**, 041604 (2000).
- [38] P. Muruganandam, R. Kishor Kumar, and S. K. Adhikari, *J. Phys. B* **43**, 205305 (2010).
- [39] P. Muruganandam and S. K. Adhikari, *J. Phys. B* **44**, 121001 (2011).
- [40] N. G. Parker, C. Ticknor, A. M. Martin, and D. H. J. O'Dell, *Phys. Rev. A* **79**, 013617 (2009).
- [41] R. M. Wilson and J. L. Bohn, *Phys. Rev. A* **83**, 023623 (2011).
- [42] M. Asad-uz-Zaman and D. Blume, *Phys. Rev. A* **83**, 033616 (2011).
- [43] D. C. E. Bortolotti, S. Ronen, J. L. Bohn, and D. Blume, *Phys. Rev. Lett.* **97**, 160402 (2006).
- [44] S. Ronen, D. C. E. Bortolotti, D. Blume, and J. L. Bohn, *Phys. Rev. A* **74**, 033611 (2006).
- [45] S. Sinha and L. Santos, *Phys. Rev. Lett.* **99**, 140406 (2007).
- [46] F. Deuretzbacher, J. C. Cremon, and S. M. Reimann, *Phys. Rev. A* **81**, 063616 (2010).
- [47] U. R. Fischer, *Phys. Rev. A* **73**, 031602 (2006).
- [48] P. Pedri and L. Santos, *Phys. Rev. Lett.* **95**, 200404 (2005).
- [49] C. Ticknor, R. M. Wilson, and J. L. Bohn, *Phys. Rev. Lett.* **106**, 065301 (2011).
- [50] R. Nath, P. Pedri, and L. Santos, *Phys. Rev. Lett.* **102**, 050401 (2009).
- [51] S. Inouye, M. R. Andrews, J. Stenger, H.-J. Miesner, D. M. Stamper-Kurn and W. Ketterle, *Nature* **392**, 151 (1998).
- [52] S. Stringari, *Phys. Rev. Lett.* **77**, 2360 (1996).